Impacts of bromine and iodine chemistry on tropospheric OH and HO_2: Comparing observations with box and global model perspectives

Daniel Stone,[1] Tomás Sherwen,[2] Mathew J. Evans,[2,3] Stewart Vaughan,[1] Trevor Ingham,[1,4] Lisa K. Whalley,[1,4] Peter M. Edwards,[2] Katie A. Read,[2,3] James D. Lee,[2,3] Sarah J. Moller,[2,3] Lucy J. Carpenter, [2,3] Alastair C. Lewis, [2,3] Dwayne E. Heard[1,4]

[1] School of Chemistry, University of Leeds, Leeds, UK
[2] Wolfson Atmospheric Chemistry Laboratories, Department of Chemistry, University of York, York, UK
[3] National Centre for Atmospheric Science, University of York, York, UK
[4] National Centre for Atmospheric Science, University of Leeds, Leeds, UK
* Now at Department of Chemistry, University of York, York, UK

Supplementary Material

Speciation of modelled peroxy radicals

Figure S1 shows the speciation of peroxy radicals during SOS determined by the box model. The dominant species at Cape Verde are HO_2 and CH_3O_2, which comprise 87.4 % of the total peroxy radical concentration, and are followed by $CH_3C(O)O_2$ (6.5 %) and $C_2H_5O_2$ (1.1 %), all of which display no HO_2 interference in the laboratory (Whalley et al., 2013; Stone et al., 2014). Any peroxy species potentially contributing to interferences in HO_2 measurements thus constitutes < 4 % of the total peroxy radical concentration, with each species representing < 1 % of the total. Potential interferences arising from conversion of alkene- and aromatic-derived peroxy radicals to OH within the LIF detection cell, as described by Fuchs et al. (2011), are thus expected to be small for SOS and are not explicitly described in the model for this work.

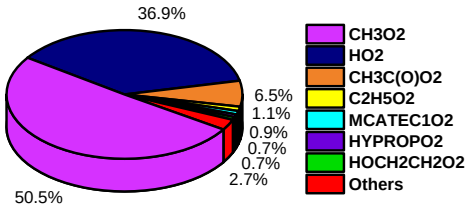

Figure S1: Speciation of peroxy radicals during SOS1 and SOS2. Radical names are as given by the MCM.

Impact of CH_3O_2 + OH

Recent experiments have indicated a rapid reaction between CH_3O_2 and OH (Bossolasco et al., 2014; Fittschen et al., 2014; Assaf et al., 2016; Yan et al., 2016), with the dominant products expected to be CH_3O + HO_2 at an observed yield of (0.8 ± 0.2) (Assaf et al., 2017). As shown in Figures 5 and 6 (main text), this reaction contributes 4 %, on average, to the total midday OH loss during SOS and 5 % to the total HO_2 production, assuming 100 % yield of CH_3O + HO_2. Inclusion of the reaction in the chemistry scheme, for model runs in which halogens are included, decreases the modelled concentration of OH at midday from 5.3 $\times 10^6$ cm^{-3} to 5.2 $\times 10^6$ cm^{-3}, and increases the HO_2 concentration from 3.2 $\times 10^8$ cm^{-3} to 3.9 $\times 10^8$ cm^{-3}.

Figure S2 shows the mean modelled diurnal profile for CH_3O_2 during SOS, for model runs with and without the reaction between CH_3O_2 and OH. Inclusion of the reaction decreases the mean midday CH_3O_2 concentration by 24 %, from 5.7 $\times 10^8$ cm^{-3} to 4.6 $\times 10^8$ cm^{-3}, and thus has a more significant impact on CH_3O_2 than on OH or HO_2. Similar changes to modelled OH, HO_2 and CH_3O_2 were reported by Assaf et al. (2017) using an updated MCM based model for the RHaMBLe campaign in Cape Verde in 2007 (Whalley et al., 2010).

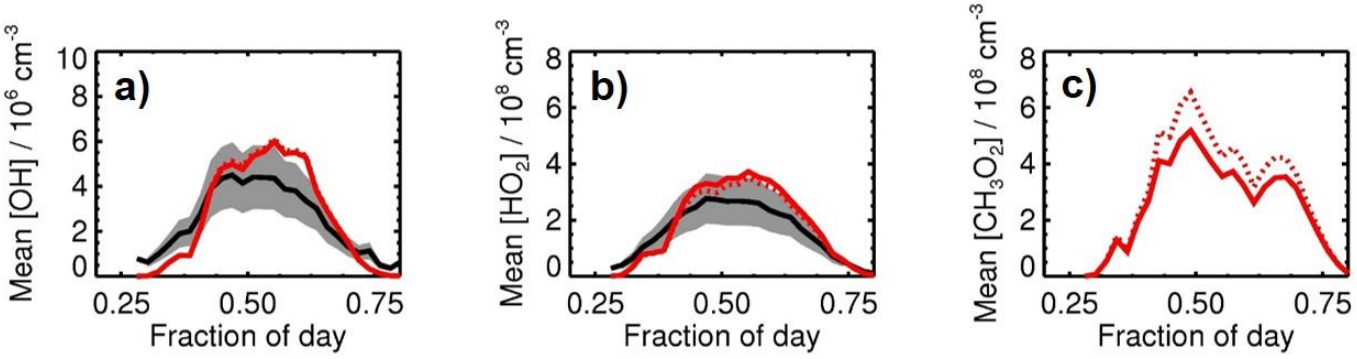

Figure S2: Mean box modelled diurnal profiles for a) OH; b) HO_2; c) CH_3O_2 during SOS (SOS1 and SOS2 combined) for model runs with (red solid line) and without (red broken line) the reaction between CH_3O_2 and OH. For OH and HO_2, observations are shown in black, with grey shading indicating the variability in the observations.

Figure S3 shows the mean midday (1100 to 1300 hours) budgets for CH_3O_2 during SOS for model runs with and without the reaction between CH_3O_2 and OH. Midday production of CH_3O_2, both with and without the reaction between CH_3O_2 and OH, is dominated by CH_3 radical production from CH_4 + OH (~ 55 %), and is followed by the reactions of $CH_3C(O)O_2$ radicals with NO (~ 17 %) and other RO_2 radicals (~ 15 %). Midday loss of CH_3O_2, when CH_3O_2 is included, is dominated by reactions with NO (~ 41 %), HO_2 (~ 33 %), the reaction with OH (~ 15 %), and CH_3O_2 self-reaction (~ 8 %). If the reaction of CH_3O_2 with OH is not included in the model, the loss

reaction with NO represents ~ 48 % of the total CH_3O_2 loss and the reactions with HO_2 and other CH_3O_2 radicals represent ~ 36 % and ~ 12 %, respectively.

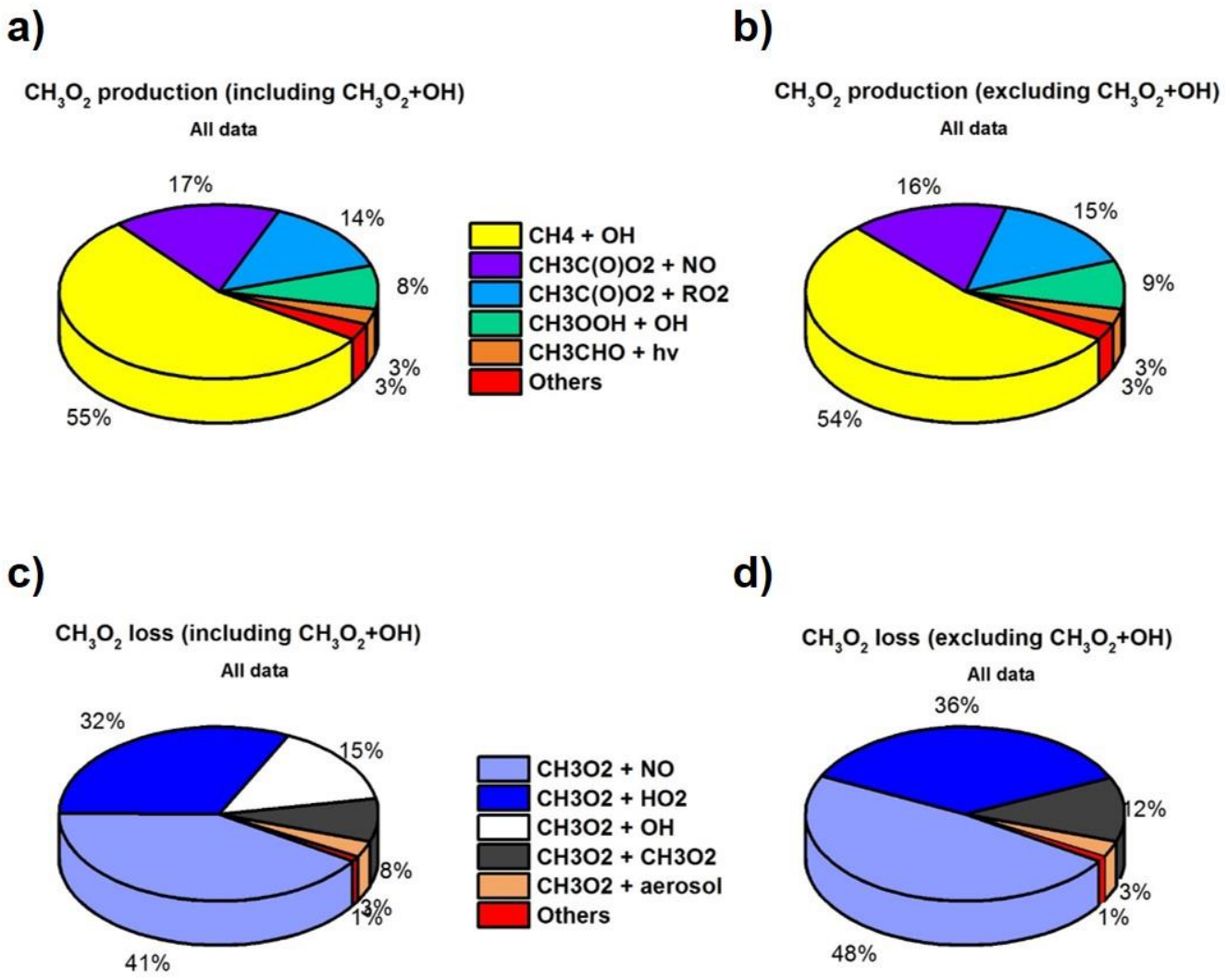

Figure S3: Mean midday (1100 to 1300 hours) budgets for CH_3O_2 during SOS (SOS1 and SOS2 combined). Panel a) production of CH_3O_2 for model runs with the reaction between CH_3O_2 and OH; b) production of CH_3O_2 for model runs without the reaction between CH_3O_2 and OH; c) loss of CH_3O_2 for model runs with the reaction between CH_3O_2 and OH; d) loss of CH_3O_2 for model runs without the reaction between CH_3O_2 and OH.

Time series for observed and box modelled OH and HO_2 radical concentrations

Figures S4 and S5 shows the times series for OH and HO_2 observations and model simulations day-by-day during SOS1 and SOS2.

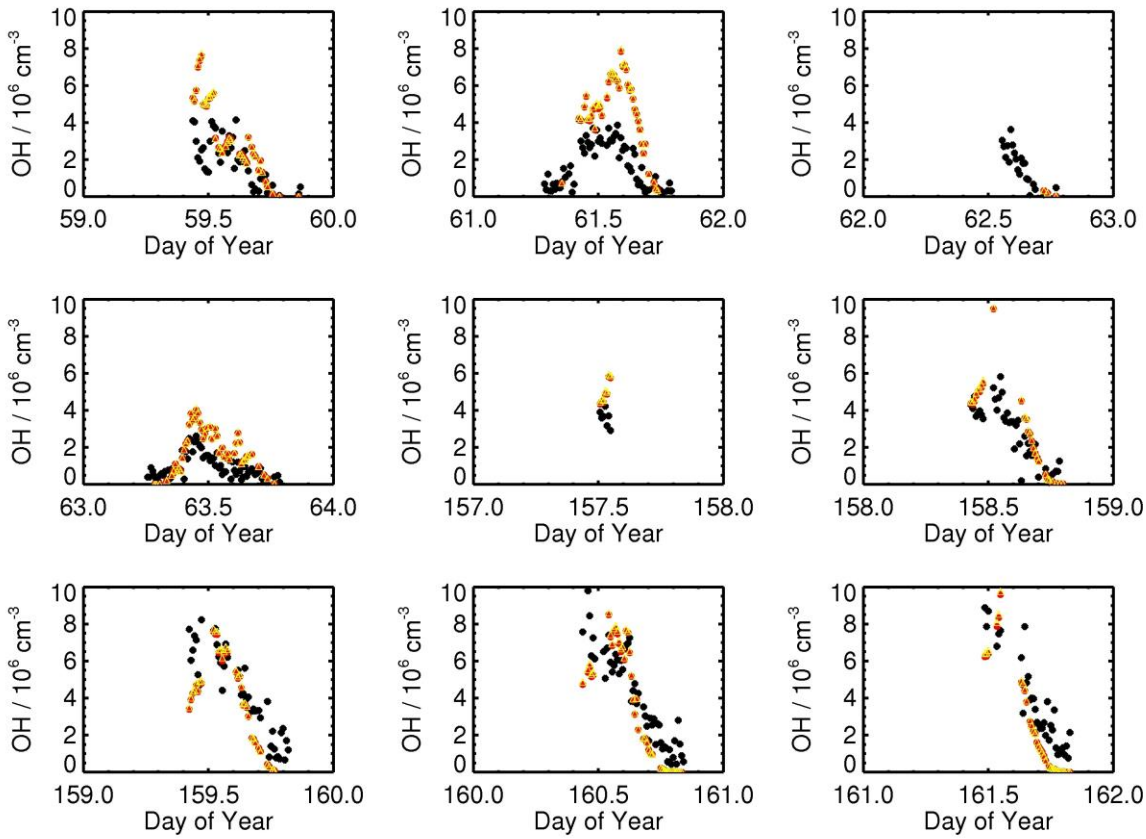

Figure S4: Times series for observed and modelled OH during SOS1 (days 59 to 63) and SOS2 (days 157 to 162). Observed data are shown in black; box model concentrations with halogen chemistry are shown by filled red circles; box model concentrations without halogen chemistry are shown by open orange triangles.

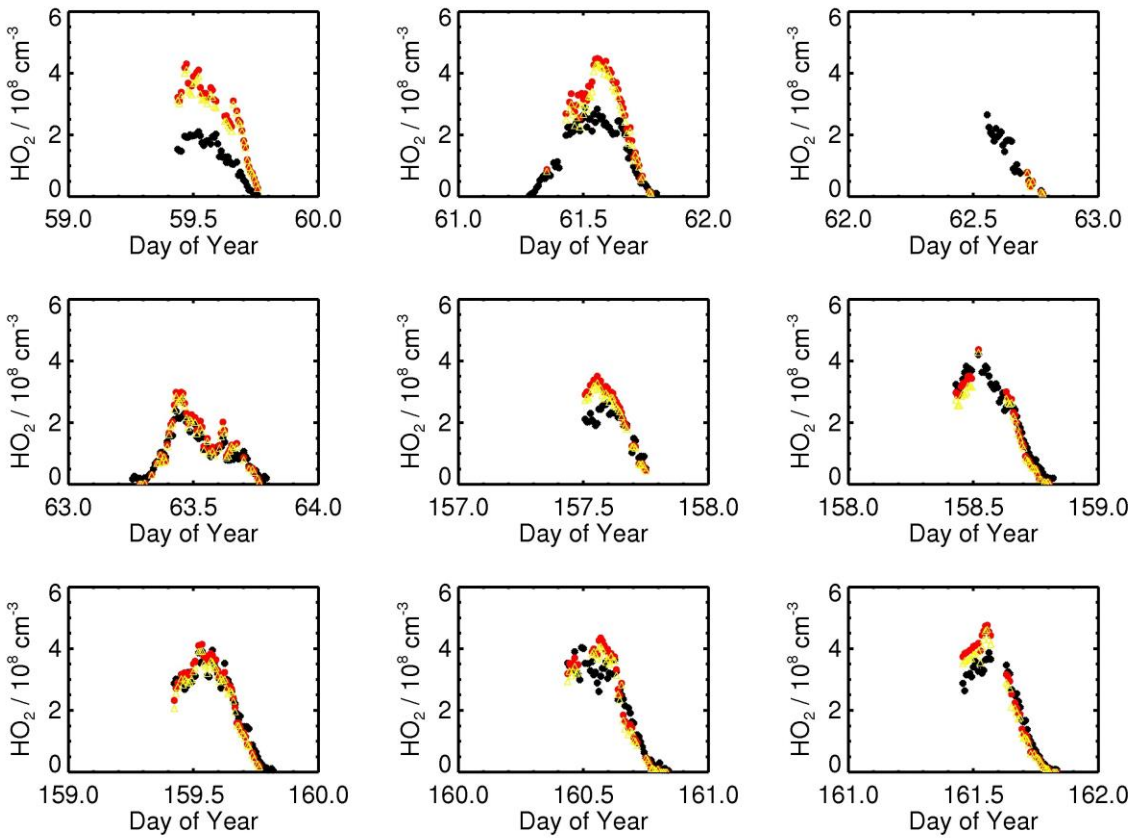

Figure S5: Times series for observed and modelled HO_2 during SOS1 (days 59 to 63) and SOS2 (days 157 to 162). Observed data are shown in black; box model concentrations with halogen chemistry are shown by filled red circles; box model concentrations without halogen chemistry are shown by open orange triangles.

References

Assaf, E., Song, B., Tomas, A., Schoemaker, C., and Fittschen, C.: Rate constant of the reaction between CH_3O_2 and OH radicals revisited, J. Phys. Chem. A, 120, 8923-8932, 2016

Assaf, E., Sheps, L., Whalley, L., Heard, D., Tomas, A., Schoemaecker, C., and Fittschen, C.: The reaction between CH_3O_2 and OH radicals: Product yields and atmospheric implications, Environ. Sci. Technol., 51, 4, 2170-2177, doi: 10.1021/acs.est.6b06265, 2017

Bossolasco, A., Farago, E.P., Schoemaker, C., and Fittschen, C.: Rate constant of the reaction between CH_3O_2 and OH radicals, Chem. Phys. Lett., 593, 7-13, 2014

Fittschen, C., Whalley, L.K., and Heard, D.E.: The reaction of CH_3O_2 radicals with OH radicals: A neglected sink for CH_3O_2 in the remote atmosphere, Environ. Sci. Technol., 118, 7700-7701, 2014

Fuchs, H., Bohn, B., Hofzumahaus, A., Holland, F., Lu, K. D., Nehr, S., Rohrer, F., Wahner, A.: Detection of HO_2 by laser induced fluorescence: calibration and interferences from RO_2 radicals, Atmos. Meas. Tech., 4, 1209–1225, 2011

Stone, D., Evans, M.J., Walker, H., Ingham, T., Vaughan, S., Ouyang, B., Kennedy, O.J., McLeod, M.W., Jones, R.L., Hopkins, J., Punjabi, S., Lidster, R., Hamilton, J.F., Lee, J.D., Lewis, A.C., Carpenter, L.J., Forster, G., Oram, D..E., Reeves, C.E., Bauguitte, S., Morgan, W., Coe, H., Aruffo, E., Dari-Salisburgo, C., Giammaria, F., Di Carlo, P., and Heard, D.E.: Radical Chemistry at Night: Comparisons between observed and modeled HO_x, NO_3 and N_2O_5 during the RONOCO project, Atmos. Chem. Phys., 14, 1299-1321, 2014, doi:10.5194/acp-14-1299-2014

Whalley, L.K., Furneaux, K.L., Goddard, A., Lee, J.D., Mahajan, A., Oetjen, H., Read, K.A., Kaaden, N., Carpenter, L.J., Lewis, A.C., Plane, J.M.C., Saltzman, E.S., Wiedensohler, A., Heard, D.E.: The chemistry of OH and HO_2 radicals in the boundary layer over the tropical Atlantic Ocean, Atmos. Chem. Phys., 10, 1555-1576, 2010

Whalley, L.K., Blitz, M.A., Desservettaz, M., Seakins, P.W., and Heard, D.E.: Reporting the sensitivity of laser-induced fluorescence instruments used for HO_2 detection to an interference from RO_2 radicals and introducing a novel approach that enables HO_2 and certain RO_2 types to be selectively measured, Atmos. Meas. Tech., 6, 3425-3440, 2013, doi:10.5194/amt-6-3425-2013

Yan, C., Kocevska, S., and Krasnoperov, L.N.: Kinetics of the reaction of CH_3O_2 radicals with OH studied over the 292-526 K temperature range, J. Phys. Chem. A, 120, 6111-6121, 2016